

Supplementary Material

The effects of drought on land cover change and vegetation productivity in continental Chile

Francisco Zambrano^{a,b,*}, Anton Vrieling^c, Francisco Meza^{d,e,f}, Iongel Duran-Llacer^g, Francisco Fernández^{h,i}, Alejandro Venegas-González^j, Nicolas Raab^d, Dylan Craven^{l,m}

^a*Hémera Centro de Observación de la Tierra, Facultad de Ciencias, Escuela de Ingeniería en Medio Ambiente y Sustentabilidad, Universidad Mayor, Santiago, 7500994, Chile.,*

^b*Observatorio de Sequía para la Agricultura y la Biodiversidad de Chile (ODES), Universidad Mayor, Santiago, 7500994, Chile.,*

^c*Faculty of Geo-Information Science and Earth, University of Twente, Enschede, The Netherlands.,*

^d*Facultad de Agronomía y Sistemas Naturales, Pontificia Universidad Católica de Chile., Santiago, Chile.,*

^e*Instituto para el Desarrollo Sustentable. Pontificia Universidad Católica de Chile, Santiago, Chile.,*

^f*Centro Interdisciplinario de Cambio Global, Pontificia Universidad Católica de Chile, Santiago, Chile.,*

^g*Hémera Centro de Observación de la Tierra, Facultad de Ciencias, Universidad Mayor., Santiago, 7500994, Chile.,*

^h*Center of Economics for Sustainable Development (CEDES), Faculty of Economics and Government, Universidad San Sebastian, Santiago, Chile.,*

ⁱ*Center of Applied Ecology and Sustainability (CAPES), Santiago, Chile.,*

^j*Instituto de Ciencias Agroalimentarias, Animales y Ambientales (ICA3), Universidad de O'Higgins, San Fernando, Chile.,*

^k,

^l, *GEMA Center for Genomics, Ecology & Environment, Universidad Mayor, Camino La Pirámide Huechuraba 5750, Santiago, Chile.,*

^m*Data Observatory Foundation, Santiago, Chile.,*

S1. Validation of ERA5L variables

S1.1. Methods

We compared the ERA5L (Muñoz-Sabater et al., 2021) variables for monthly mean temperature, total precipitation, and volumetric soil water content against values retrieved by weather stations. For temperature and precipitation, we used data from the weather network from the Ministry of Agriculture of Chile (www.agromet.com) between 2015 and 2023. We used 277 stations located throughout Chile. For *in-situ* soil moisture, we used a private soil network that is owned by the agricultural enterprise Garces Fruit (<https://garcesfruit.com/>), which has 99 stations in Central Chile, located in fields with cherry fruit crops. The sensors are installed at 30, 60, and 90cm and are a Advanced Soil Moisture Sensor model Teros 12 from the METER Group (<https://metergroup.com/products/teros-12/>). To avoid comparing ERA5L with *in-situ* soil moisture levels caused by irrigation, which are not captured by ERA5L, we used daily data for the year 2022 and the months outside the growing season, May to September.

*Corresponding author

Email address: francisco.zambrano@umayor.cl (Francisco Zambrano)

We selected the following metrics:

$$\begin{aligned}
MAE &= \frac{1}{n} \sum |E - S| \\
Bias &= \frac{\sum E}{\sum S} \\
ubRMSE &= \sqrt{\frac{\sum [(E_i - \bar{E}) - (S_i - \bar{S})]^2}{n}} \\
CC &= \frac{\sum (S_i - \bar{S})(E_i - \bar{E})}{\sqrt{(\sum (S_i - \bar{S})^2)(\sum (E_i - \bar{E})^2)}}
\end{aligned}$$

MAE: mean absolute error

bias: bias

ubRMSE: unbiased root mean squared error

CC: coefficient of correlation

S: value of the variable measure by the weather station

E: value of the variable measure by ERA5L

S1.2. Results

The average performance metrics of ERA5L over the 266 weather stations is shown in ?

In the case of the 97 soil moisture stations, we averaged for the three depths (30, 60, and 90cm) and then compared it with the volumetric water content in the top 100cm of the soil derived from ERA5L. For this case, we made a daily comparison to determine the performance metrics per station, then we averaged the measured soil moisture at the three levels and over all stations.

Table S1: Metrics of performance for the climatic and soil moisture variables from ERA5-Land with data from 266 stations in Central Chile.

Variable	ubRMSE	MAE	Bias	CC
Temperature	1.06°C	1.131°C		0.96
Precipitation		28.1mm	1.93	0.845
Soil Moisture (1m)	0.174 cc/cc	0.167 cc/cc	1.74	0.71

S2. Land cover macroclasses and validation

S2.1. Methods

To analyze the LULCC, we used the IGBP scheme from the MCD12Q1 Collection 6.1 from MODIS. This product has a yearly frequency from 2001 to 2022. The IGBP defines 17 classes; we regrouped these into ten macroclasses, as follows: classes 1-4 to forest, 5-7 to shrublands, 8-9 to savannas, 10 as grasslands, 11 as wetlands, 12 and 14 to croplands, 13 as urban, 15 as snow and ice, 16 as barren, and 17 to water bodies.

To assess the accuracy of the regrouped MCD12Q1 land cover maps, we compared the macroclasses with those of a more detailed land cover map made by [Zhao et al. \(2016\)](#) for Chile with samples acquired in the years 2013–2014 (LCChile). The latter has a spatial resolution of 30 m and three hierarchy levels of defined classes; from those, we used level 1, which fits with the macroclass land cover. We chose the years 2013 (IGBP2013) and 2014 (IGBP2014) from the land cover macroclasses to compare with LCChile. For this comparison, we used the following procedure:

- i) we resampled LCChile to the spatial resolution (500m) of the land cover macroclasses using the majority method,
- ii) we took a random sample of 1000 points within continental Chile and extracted the classes that fell within each point for LCChile, IGBP2013, and IGBP2014; we considered the point extracted from LCChile as the truth and the values from the other two years as predictions.
- iii) we derived a confusion matrix with the classes extracted from the 1000 points for LCChile, IGBP2013, and IGBP2014; and calculated the performance metrics of accuracy and F1.

$$Accuracy = \frac{TP + TN}{TP + TN + FP + FN} = \frac{\text{correct classifications}}{\text{all classifications}}$$

$$F1 = \frac{2 \cdot TP}{2 \cdot TP + FP + FN}$$

where TP and FN refer to true positive and false negative, correctly classified classes; TN and FP to true negative and false positive, wrongly classified classes.

S2.2. Results

Our results showed a global accuracy of ~0.82 and a F1 score of ~0.66 between the high resolution landcover (LCChile) and the landcover IGBP from MODIS. Thus, for vegetation, we obtained and use hereafter five macroclasses of land cover from IGBP MODIS: forest, shrubland, savanna, grassland, and croplands (Table S2).

Table S2: Landcover classes from IGBP MODIS and the corresponding macroclasses.

Name	Value	Description	Macroclass
Evergreen Needleleaf Forests	1	Dominated by evergreen conifer trees (canopy >2m). Tree cover >60%.	Forest
Evergreen Broadleaf Forests	2	Dominated by evergreen broadleaf and palmate trees (canopy >2m). Tree cover >60%.	Forest
Deciduous Needleleaf Forests	3	Dominated by deciduous needleleaf (larch) trees (canopy >2m). Tree cover >60%.	Forest
Deciduous Broadleaf Forests	4	Dominated by deciduous broadleaf trees (canopy >2m). Tree cover >60%.	Forest
Mixed Forests	5	Dominated by neither deciduous nor evergreen (40-60% of each) tree type (canopy >2m). Tree cover >60%.	Forest
Closed Shrublands	6	Dominated by woody perennials (1-2m height) >60% cover.	Shrublands
Open Shrublands	7	Dominated by woody perennials (1-2m height) 10-60% cover.	Shrublands
Woody Savannas	8	Tree cover 30-60% (canopy >2m).	Savanna
Savannas	9	Tree cover 10-30% (canopy >2m).	Savanna
Grasslands	10	Dominated by herbaceous annuals (<2m).	Grassland
Permanent Wetlands	11	Permanently inundated lands with 30-60% water cover and >10% vegetated cover.	Wetland
Croplands	12	At least 60% of area is cultivated cropland.	Cropland
Urban and Built-up Lands	13	At least 30% impervious surface area including building materials, asphalt, and vehicles.	Urban
Cropland/Natural Vegetation Mosaics	14	Mosaics of small-scale cultivation 40-60% with natural tree, shrub, or herbaceous vegetation.	Cropland
Permanent Snow and Ice	15	At least 60% of area is covered by snow and ice for at least 10 months of the year.	Snow/ice
Barren	16	At least 60% of area is non-vegetated barren (sand, rock, soil) areas with less than 10% vegetation	Barren land
Water Bodies	17	At least 60% of area is covered by permanent water bodies	Water
Unclassified	255	Has not received a map label because of missing inputs	Unclassified

S3. Relationship between drought indices and land cover change

Figure S1 shows the ranking of variable importance obtained with the ten folds used in the resampling of the Random Forest model per land cover type.

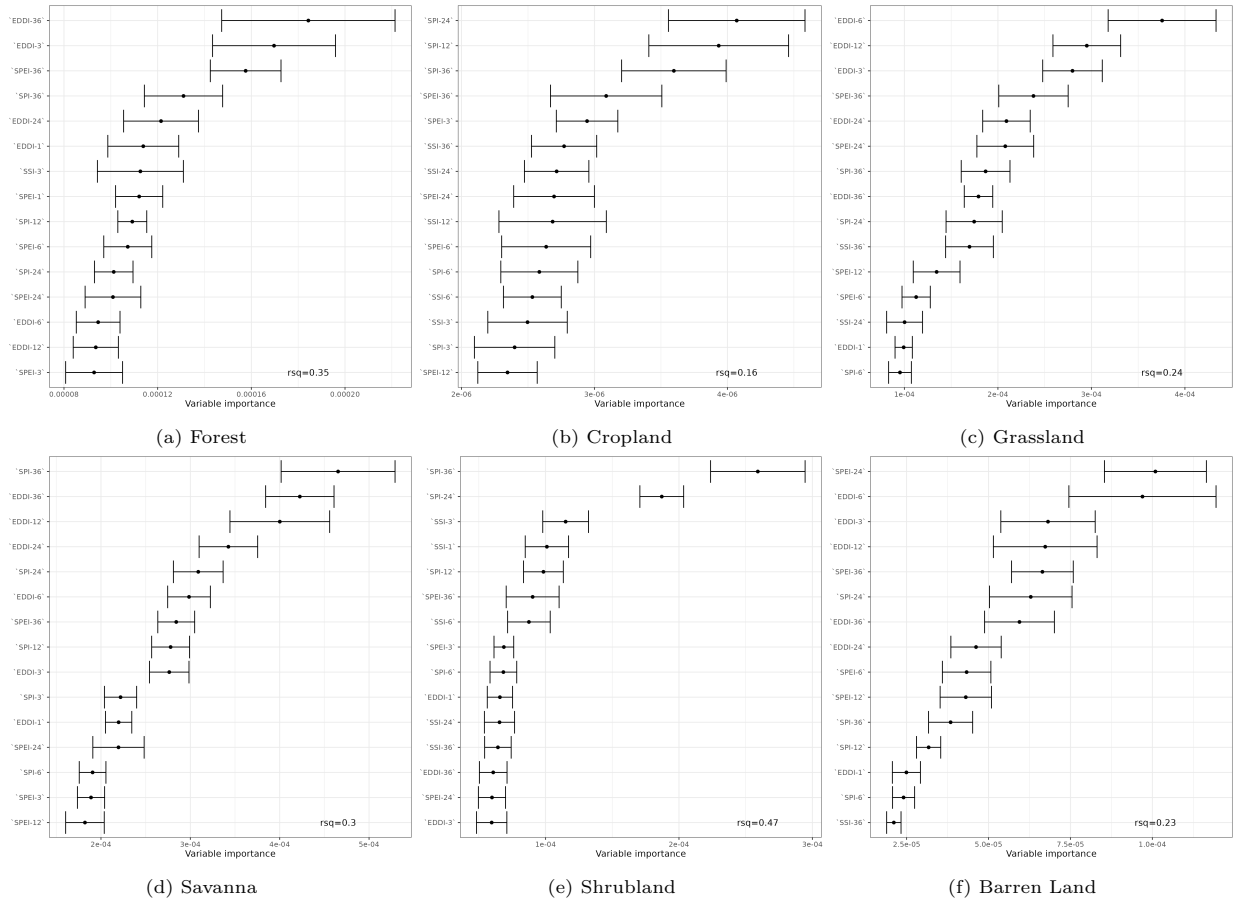


Figure S1: Error bar for the variables importance obtained from the 10 resamples folded by the Random Forest used to model land cover trend using as predictors the trend in drought indices of water supply, water demand, soil moisture, and vegetation productivity.

S4. Trend of vegetation productivity

Figure S2 shows the average trend for zcNDVI for 2000-2023 per macrozone and landcover macroclass.

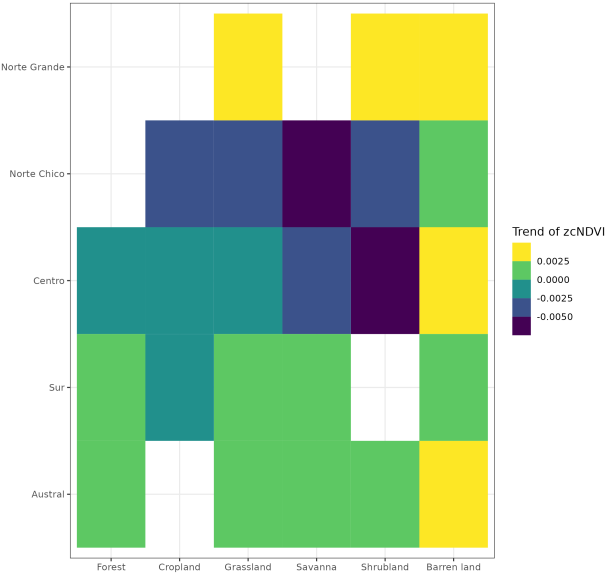


Figure S2: Heatmap of trends in zcNDVI for 2000 to 2023 per macrozone and landcover macroclass.

S5. Vegetation productivity

We analyzed the correlation of zcNDVI for time scales of 1, 3, 6, and 12 months versus net primary production (NPP). We obtained both the zcNDVI from MOD13A3.061 and the NPP from MOD17A3HGF.061, using MODIS products. We used the zcNDVI in December to correlate with the annual NPP. Figure S3 shows a map of the r-squared correlation between zcNDVI and NPP, and Figure S4 shows the aggregated values per macrozone.

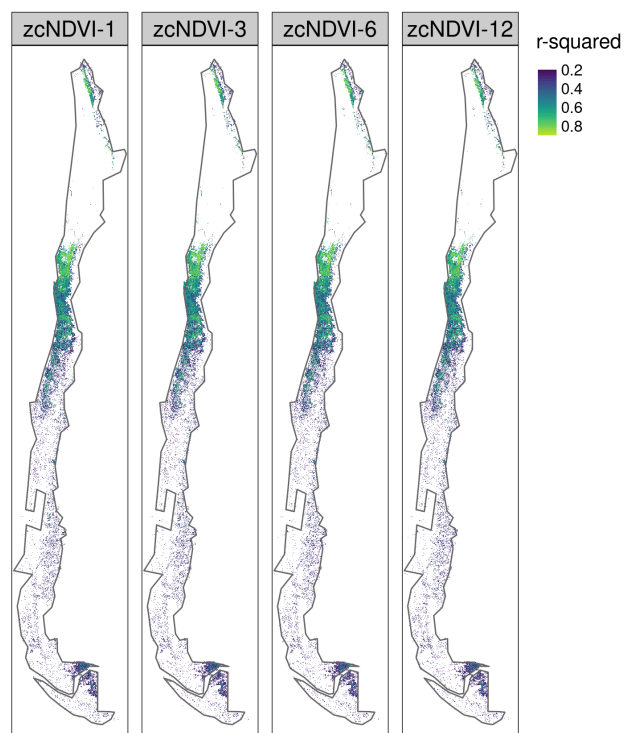


Figure S3: Spatial variation of the r-squared values obtained from the yearly correlation of zcNDVI of 1, 3, 6, and 12 months with the net primary productivity (NPP) for continental Chile.

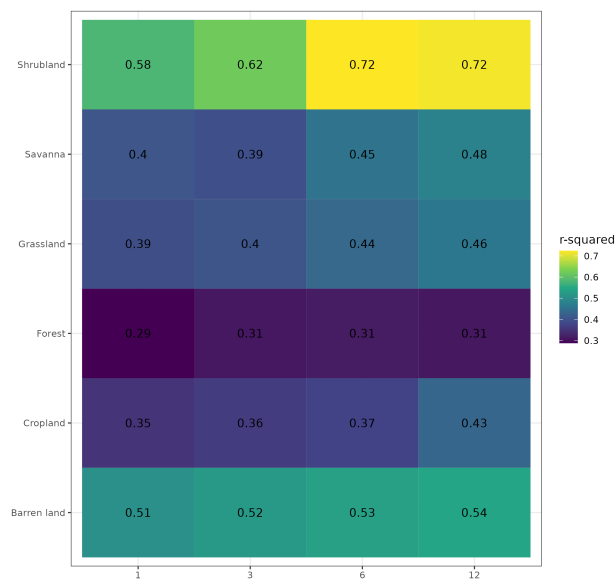


Figure S4: A heatmap showing the r-squared values obtained from the yearly correlation of zcNDVI of 1, 3, 6, and 12 months with the net primary productivity (NPP) for continental Chile.

References

- Muñoz-Sabater, J., Dutra, E., Agustí-Panareda, A., Albergel, C., Arduini, G., Balsamo, G., Boussetta, S., Choulga, M., Harrigan, S., Hersbach, H., Martens, B., Miralles, D.G., Piles, M., Rodríguez-Fernández, N.J., Zsoter, E., Buontempo, C., Thépaut, J.N., 2021. ERA5-Land: a state-of-the-art global reanalysis dataset for land applications. *Earth System Science Data* 13, 4349–4383. URL: <https://essd.copernicus.org/articles/13/4349/2021/>, doi:10.5194/essd-13-4349-2021.
- Zhao, Y., Feng, D., Yu, L., Wang, X., Chen, Y., Bai, Y., Hernández, H.J., Galleguillos, M., Estades, C., Biging, G.S., Radke, J.D., Gong, P., 2016. Detailed dynamic land cover mapping of Chile: Accuracy improvement by integrating multi-temporal data. *Remote Sensing of Environment* 183, 170–185. URL: <https://linkinghub.elsevier.com/retrieve/pii/S0034425716302188>, doi:10.1016/j.rse.2016.05.016.